

Superdeformation in bismuth

R. M. Clark,¹ S. Bouneau,² A. N. Wilson,³ B. Cederwall,¹ F. Azaiez,² S. Asztalos,¹ J. A. Becker,⁴ L. Bernstein,⁴ M. J. Brinkman,⁵ M. A. Deleplanque,¹ I. Deloncle,⁶ R. M. Diamond,¹ J. Duprat,² P. Fallon,¹ L. P. Farris,⁴ E. A. Henry,⁴ J. R. Hughes,⁴ W. H. Kelly,⁷ I. Y. Lee,¹ A. O. Macchiavelli,¹ M. G. Porquet,⁶ J. F. Sharpey-Schafer,³ F. S. Stephens,¹ M. A. Stoyer,¹ and D. T. Vo⁴

¹Lawrence Berkeley Laboratory, 1 Cyclotron Road, Berkeley, California 94720

²IPN, IN2P3-CNRS, Bâtiment 104, F-91406 Orsay Cedex, France

³Oliver Lodge Laboratory, University of Liverpool, Liverpool, L69 3BX, United Kingdom

⁴Lawrence Livermore National Laboratory, Livermore, California 94550

⁵Oak Ridge National Laboratory, Oak Ridge, Tennessee 37831

⁶CSNSM, IN2P3-CNRS, Bâtiment 104-108, F-91405 Orsay Cedex, France

⁷Iowa State University, Ames, Iowa 50011

(Received 3 May 1995)

High angular momentum states in $^{195-197}\text{Bi}$ are populated in two reactions: $^{183}\text{W}(^{19}\text{F},xn)^{202-x}\text{Bi}$ and $^{181}\text{Ta}(^{20}\text{Ne},xn)^{201-x}\text{Bi}$ at beam energies of 108 and 123 MeV, respectively. Gamma rays were detected using the Gammasphere array. Three weakly populated rotational sequences have been found. They each have properties characteristic of other superdeformed bands in this mass region. On the basis of cross-bombardment information we believe that one band belongs to each of ^{195}Bi , ^{196}Bi , and ^{197}Bi . The properties of the bands in the odd-Bi nuclei are best reproduced if the odd proton occupies the favored signature of the $[651]1/2$ orbital, while the band in ^{196}Bi has this same proton configuration coupled to an additional $N=7$ ($j_{15/2}$) neutron. The relative behavior of the $\mathcal{J}^{(2)}$ moments of inertia can be qualitatively understood in terms of Pauli-blocking effects.

PACS number(s): 21.10.Re, 27.80.+w, 23.20.Lv

I. INTRODUCTION

Superdeformation in the mass-190 region was first observed in ^{191}Hg [1], and since then over 40 superdeformed (SD) bands have been found in the Au, Hg, Tl, and Pb nuclei [2]. A striking difference between the SD nuclei of the $A\sim 190$ region and those in other mass regions is in the behavior of the dynamic moment of inertia $\mathcal{J}^{(2)}$ as a function of rotational frequency ω . SD bands in nuclei of the lighter $A\sim 130$ and $A\sim 150$ mass regions have $\mathcal{J}^{(2)}$'s which display pronounced differences from nucleus to nucleus, while the majority of bands in the $A\sim 190$ region shows the same smooth rise in $\mathcal{J}^{(2)}$. This behavior of $\mathcal{J}^{(2)}$ has been interpreted [3,4] as resulting from the gradual alignments of pairs of nucleons occupying specific high- N intruder orbitals (namely, $j_{15/2}$ neutrons and $i_{13/2}$ protons) in the presence of weak pair correlations. In this picture, Pauli blocking of high- N intruder orbitals should flatten the $\mathcal{J}^{(2)}$. In the odd-odd Tl isotopes blocking of both the intruder quasiproton and quasineutron alignments (double blocking) has been suggested as the mechanism responsible for the reduced $\mathcal{J}^{(2)}$ slope observed for some of the bands [5,6]. In the odd-Hg [7,8] and odd-Pb [9,10] nuclei single blocking of the $N=7$ quasineutron alignments is thought to be responsible for flattening the $\mathcal{J}^{(2)}$ of some bands.

Many theoretical calculations (see, e.g., [11–13]) predict well-defined secondary SD minima persisting in the bismuth and polonium nuclei. However, until recently no superdeformed bands, in the $A\sim 190$ region, had been found in nuclei with $Z>82$. In an earlier Rapid Communication [14] we

gave a preliminary report of part of this work and described two new SD bands which could be unambiguously assigned to the Bi nuclei. This observation represented confirmation of these long-standing predictions. It should also be noted that a candidate for a SD band in ^{198}Po has recently been reported [15]. In this follow-up paper we describe results from two experiments aimed at investigating superdeformation in $^{195-197}\text{Bi}$. In addition to the two bands reported in [14], a third SD band has been found. The isotopic and configuration assignments of these bands are discussed. Cranked Woods-Saxon calculations are presented and it is shown that the relative behavior of the $\mathcal{J}^{(2)}$'s for these bands can be qualitatively understood in terms of Pauli-blocking effects. Our results provide important information on the nature of the proton orbitals above $Z=82$ at large deformation ($\beta_2\approx 0.48$).

II. EXPERIMENTAL DETAILS

Two reactions were used to populate high-spin states in $^{195-197}\text{Bi}$. The beams were provided by the 88-Inch Cyclotron facility at the Lawrence Berkeley Laboratory. Gamma rays were detected with the Gammasphere array [16] which, for these experiments, comprised 36 Compton-suppressed, large-volume (photopeak efficiency $\sim 75-85\%$ at 1332 keV) HPGe detectors. Fifteen detectors were situated at forward angles, 15 at backward angles, and the other 6 at 90° relative to the beam axis. The first reaction was

$$^{183}\text{W}(^{19}\text{F},xn), \quad E_b = 108 \text{ MeV}. \quad (1)$$

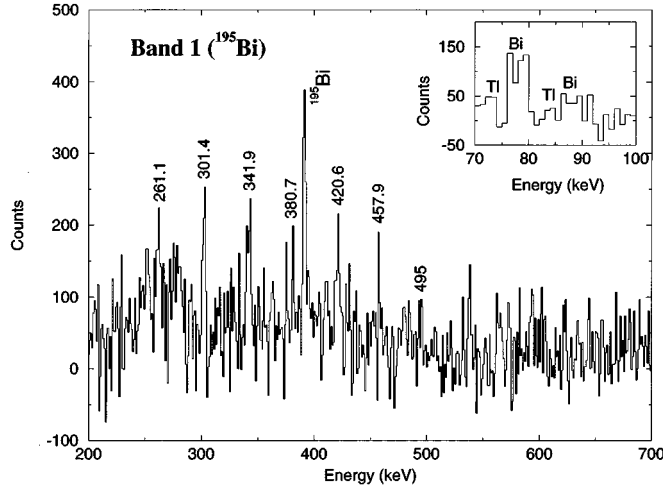
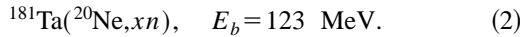


FIG. 1. A sum of double-gated spectra from threefold coincidence data for band 1. The gates used were of varying widths and they included all members of the band except the 420.6 keV γ ray. The transition energies are given in keV. The transition marked “ ^{195}Bi ” is the known 391.7 keV ($17/2^+ \rightarrow 15/2^-$) γ ray in ^{195}Bi (see text). The inset shows the region of the spectrum around the x rays. The approximate position of Bi and Tl K_α and K_β x ray lines is indicated.

It was aimed at populating states in $^{196,197}\text{Bi}$. The target consisted of $2 \times 300 \mu\text{g cm}^{-2}$ stacked ^{183}W foils mounted on thin carbon backings. A total of 8×10^8 three- and higher-fold events were collected. The second reaction was



It was aimed at populating states in $^{195,196}\text{Bi}$. The target consisted of $2 \times 350 \mu\text{g cm}^{-2}$ self-supporting ^{181}Ta foils. A total of 9×10^8 three- and higher-fold events were collected. The data were analyzed off line by sorting events in $E_{\gamma_1}-E_{\gamma_2}-E_{\gamma_3}$ cubes and gated $E_{\gamma_1}-E_{\gamma_2}$ matrices.

III. RESULTS

In total, three sequences of γ rays, with properties characteristic of SD bands in this mass region, have been observed. Spectra showing the bands are presented in Figs. 1–3. In each case the spectra were formed using combinations of double gates on threefold coincidence data. A global background subtraction was taken using a fraction of the total projection. This method was found to be consistently better than using a local background subtraction. The transition energies and relative intensities of the sequences are summarized in Table I. Before discussing each of the bands in detail a few general comments should be made.

The relative intensities of the in-band transitions (see Table I) show behavior similar to all the SD bands in the $A \sim 190$ region. The band is populated over a few transitions at the top before reaching a region in which the feeding is complete and the in-band intensity is constant. The band rapidly depopulates from the lowest one or two observed states. This behavior, combined with the observed similarities of the transition energies to SD bands in neighboring nuclei, led to the conclusion that the new sequences are SD bands. Because of insufficient statistics (largely because of the low

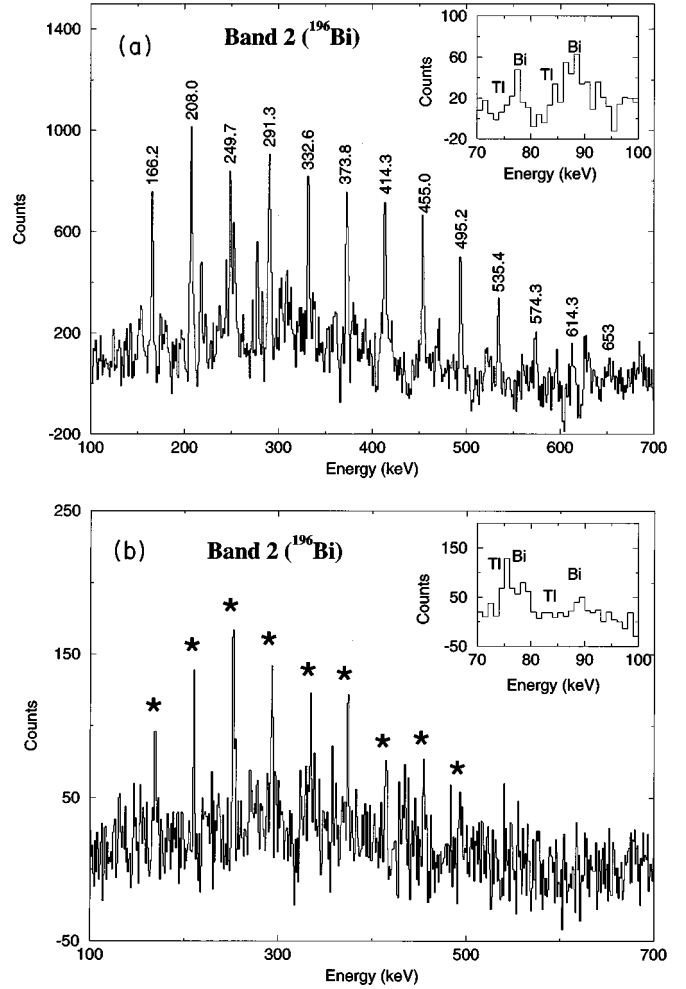


FIG. 2. (a): A sum of double-gated spectra from threefold coincidence data for band 2 formed using data from reaction (1). (b) A sum of double-gated spectra from threefold coincidence data for band 2 formed using data from reaction (2). The gates used were of varying widths and they included all band members up to the 495.2 keV γ ray. The inset shows the region of the spectrum around the x rays.

number of detectors at 90°), it has proved impossible to perform a directional correlation analysis to determine the multiplicities of the in-band transitions for any of the new sequences.

Unfortunately, the decay schemes for low-lying states in $^{195-197}\text{Bi}$ are not well known [17–19]. In addition, there are long-lived isomers at low spin in these neutron-deficient Bi isotopes. A particular problem comes with ^{196}Bi since only two γ rays are known [18], both of which deexcite isomeric states. Since both our reactions used thin targets, it was not possible to empirically determine the relative populations of the open channels in each reaction. Statistical model calculations were used to predict the dominant open channels. For reaction (1) the four most populated channels were ^{197}Bi (54%), ^{196}Bi (28%), ^{194}Tl (7%), and ^{193}Tl (4%). Similarly for reaction (2) the four dominant channels were ^{195}Bi (46%), ^{196}Bi (26%), ^{193}Tl (12%), and ^{192}Tl (6%). Generally, what was observed in the experiment was in fair agreement with the predictions although the charged particle channels may have been underestimated in the calculations. It

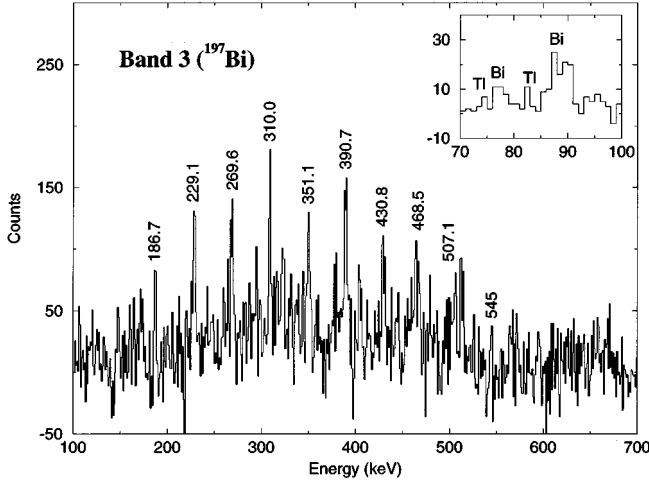


FIG. 3. A sum of double-gated spectra from threefold coincidence data for band 3. The gates used were of varying widths and included all members of the band except the 269.6, 310.0, and 507.1 keV γ rays. The transition energies are given in keV. The inset shows the region of the spectrum around the x rays.

was found empirically that no ^{195}Bi lines could be seen in data from reaction (1), while no lines from ^{197}Bi could be seen in the data from reaction (2). ^{193}Tl was populated in both reactions and known energies of ^{193}Tl yrast transitions [20] were used to check the relative energy calibrations of the data.

Consistent coincidences with Bi x rays were established for each of the bands. This is demonstrated by the insets in Figs. 1–3 which show the region of each spectrum around the x rays. Note that in the first experiment Ta absorbers were in front of the detectors while for the second experiment the absorbers were removed to facilitate detection of the x rays. Hence for Figs. 1 and 2(b) the lines associated with the lower energy K_α x rays have larger intensity than the lines associated with the K_β lines.

TABLE I. Energies and relative in-band intensities (corrected for detection efficiency and internal conversion) for the three SD bands. Energies are given in keV.

Band 1		Band 2		Band 3	
E_γ	I	E_γ	I	E_γ	I
		166.2(3)	80(10)	186.7(5)	66(7)
261.5(5)	104(10)	208.0(3)	101(5)	229.1(5)	109(10)
301.4(5)	93(10)	249.7(3)	96(5)	269.6(5)	103(10)
341.9(5)	104(10)	291.3(3)	109(7)	310.0(5)	94(10)
380.7(5)	100(10)	332.6(3)	91(5)	351.1(5)	98(10)
420.6(5)	96(10)	373.8(3)	103(5)	390.7(5)	97(10)
457.9(5)	84(10)	414.3(3)	85(5)	430.8(5)	87(8)
495(1)	33(8)	455.0(3)	89(5)	468.5(5)	46(8)
		495.2(3)	81(5)	507.1(5)	56(8)
		535.4(3)	70(5)	(545)	–
		574.3(3)	46(5)		
		614.3(5)	42(5)		
		653(1)	19(5)		

A. Band 1

A spectrum of this previously unobserved band is shown in Fig. 1. It consists of seven mutually coincident transitions (see Table I). This band was only seen in data from reaction (2). The known 391.7 keV ($17/2^+ \rightarrow 15/2^-$) transition of ^{195}Bi [17] is seen consistently in spectra formed using a variety of combinations of gates on the band members. However, the intensity of this line is always larger than the in-band intensity, possibly suggesting contamination of gates. The large intensity of the 392 keV γ ray can be seen clearly in Fig. 1. From the above information we favor the assignment of this band to ^{195}Bi . We estimate that the band has an intensity of $\sim 0.7\%$ relative to the intensity of the known 888 keV ($13/2^+ \rightarrow 9/2^-$) transition in ^{195}Bi [17]. This transition is thought to take 100% of the total channel strength, but the transition lies below several isomers and we may not be seeing the full intensity of this line in our data. Therefore, the figure of 0.7% should be regarded as an upper limit on the SD band intensity. No strongly coupled signature partner to this band could be found in the data.

B. Band 2

This band was previously reported [14] and tentatively assigned to ^{197}Bi . This assignment was based solely on analysis of the data from reaction (1). However, we also see this band in the data from reaction (2). Spectra formed from both sets of data are presented in Fig. 2. Using the common calibration to ^{193}Tl lines we find the energies of transitions from the two sets of data have a rms deviation of less than 0.7 keV. On the basis of this observation, we conclude that we are seeing only one band in the two data sets (not two ‘identical’ bands, although this possibility cannot be completely ruled out) and that it belongs to ^{196}Bi (the only Bi isotope populated appreciably in both reactions).

This is the strongest band populated in both sets of data. Note that a spectrum of this band formed from triple gates on quadruples data from reaction (1) can be seen in Fig. 1(a) of [14], and shows the topmost transitions more clearly. The other bands were too weak to be seen in a quadruples analysis. Using spectra formed under similar gating conditions we find that the band has ~ 1.5 times the intensity of band 1 as seen in the data from reaction (2), and ~ 1.9 times the intensity of band 3 as seen in the data from reaction (1) (see below). Therefore, if we assume that the different channels are populated as predicted by the statistical model calculations, then this band has an upper limit on its intensity of $\sim 2\%$ of the ^{196}Bi channel. No strongly coupled signature partner to this band could be found, although it should be noted that band 3 starts close to the half-points of the band (see Table I) but increasingly deviates from them at higher transition energies.

C. Band 3

This band was also previously reported [14] and tentatively assigned to ^{197}Bi . A spectrum of the band is presented in Fig. 3. Since it is only seen in the data from reaction (1), we still favor the assignment of this band to ^{197}Bi . However, no coincidences with known ^{197}Bi lines [19] could be established, and the assignment to ^{197}Bi must remain tentative.

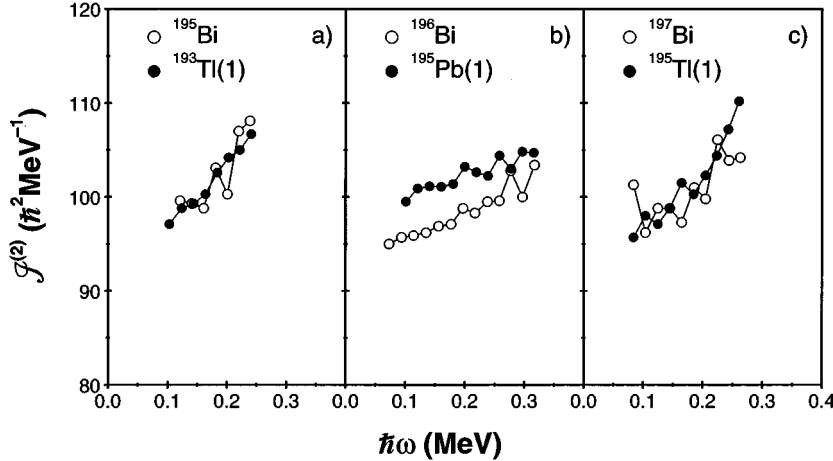


FIG. 4. Plot of the $\mathcal{J}^{(2)}$ moments of inertia as a function of rotational frequency for (a) band 1 (^{195}Bi) and $^{193}\text{Tl}(1)$, (b) band 2 (^{196}Bi) and $^{195}\text{Pb}(1)$, (c) band 3 (^{197}Bi) and $^{195}\text{Tl}(1)$.

We estimate that the upper limit of the intensity of this band is $\sim 0.6\%$ relative to the known 405 keV ($17/2^+ \rightarrow 13/2^+$) transition in ^{197}Bi [19]. This transition takes 100% of the total channel intensity, but again isomers lie above this transition and we may not be seeing the full intensity of this line. No strongly coupled signature partner band could be found.

IV. DISCUSSION

Figure 4 shows plots of the $\mathcal{J}^{(2)}$ moments of inertia for the bands and also those for several known SD bands in nearby nuclei. Bands 1 (^{195}Bi) and 3 (^{197}Bi) have $\mathcal{J}^{(2)}$'s which are of a very similar magnitude and slope to those of bands in their odd-Tl isotones [21,22] (^{193}Tl and ^{195}Tl , respectively). The transition energies of band 1 (^{195}Bi) are offset by a roughly constant amount (+7(2) keV) from band 1 in ^{193}Tl , while band 3 (^{197}Bi) has “identical” transition energies (to within ± 2 keV) of band 1 in ^{195}Tl . Band 1 (^{195}Bi) also has transition energies close to those of a band in ^{194}Pb (band 2b using the nomenclature of [23]). The relationships between the bands described above are illustrated in Fig. 5 which plots the differences in transition energies for the different pairs of bands as functions of rotational frequency. We do not intend

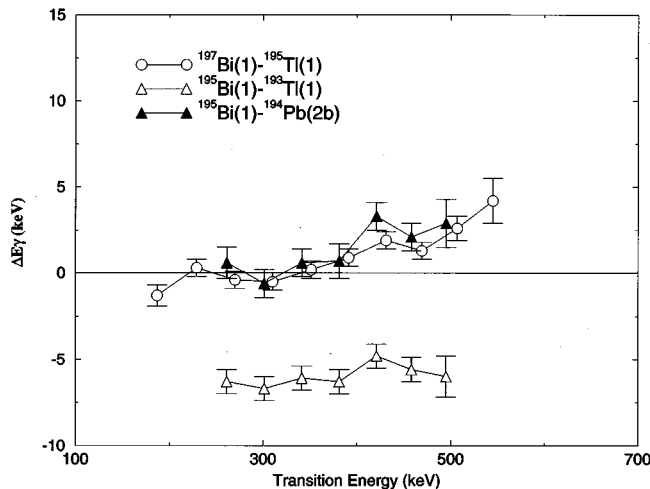


FIG. 5. Plots showing the difference in transition energies between (a) band 3 (^{197}Bi) and $^{195}\text{Tl}(1)$ (open circles), (b) band 1 (^{195}Bi) and $^{193}\text{Tl}(1)$ (open triangles), (c) band 1 (^{195}Bi) and $^{194}\text{Pb}(2b)$ (solid triangles).

to discuss the occurrence of “identical” SD bands (which is a topic of considerable current interest; see, e.g., [24–26]); we simply wish to point out that the phenomenon extends into the Bi isotopes. Band 2 (^{196}Bi) has a $\mathcal{J}^{(2)}$ which has a reduced slope when compared with that of any of the other bands for frequencies above $\omega \sim 0.2 \text{ MeV} \hbar^{-1}$. However, it is of a comparable magnitude to the other bands and still displays a rise with increasing ω .

The configuration of a SD band in an odd-Bi nucleus may be thought of in terms of an additional proton coupled to the neighboring even-Pb SD core. Figure 6(a) presents a single-particle Woods-Saxon calculation [27] for protons with deformation parameters $\beta_2=0.48$, $\beta_4=0.07$, and $\gamma=0^\circ$ (a representative deformation for SD bands in the $A \sim 190$ region; the values come from the calculations described in [12]). The calculation indicates that the $[514]9/2$ and $[651]1/2$ orbitals lie just above the $Z=82$ subshell closure. Pairing plays an important role in determining the behavior of SD bands in the $A \sim 190$ region. Presented in Fig. 6(b) is a quasiproton Routhian diagram calculated for the parameters $\beta_2=0.48$, $\beta_4=0.07$, $\gamma=0^\circ$, and $\Delta_p=\Delta_{\text{BCS}}(\omega=0)$. The calculation indicates that the $[642]5/2$, $[514]9/2$, and $[651]1/2$ are all possible one-quasiproton excitations.

The $[642]5/2$ ($i_{13/2}$) quasiparticle excitation is predominantly “holelike” in character. It is below the $Z=82$ subshell gap in the unpaired picture [see Fig. 6(a)] but with the introduction of pairing, and hence a smearing of the Fermi surface, it becomes a feasible orbital for a quasiparticle excitation. Note that, although the calculations presented here suggest that it is a low one-quasiproton excitation, changes in the nature and strength of the pairing and in the position of the proton Fermi level could change the excitation energy appreciably. Indeed, we find that with small changes in the chemical potential λ and in the pair gap Δ the relative positions of the $[642]5/2$ and $[651]1/2$ orbitals can be inverted [see Fig. 3(b) of [14]]. The implication of this is that it is not possible to be certain which orbital is lowest in energy.

Signature-partner pairs of bands based on the $[642]5/2$ orbital are observed in $^{193,195}\text{Tl}$ [21,22,28,29]. Each band in the pair is populated with similar intensity and strong dipole cross talk between the signature-partner bands is observed [28,29]. The weakness of the bands as seen in the present data means that one would not reasonably expect to see evidence of cross-talking bands. However, one would expect to

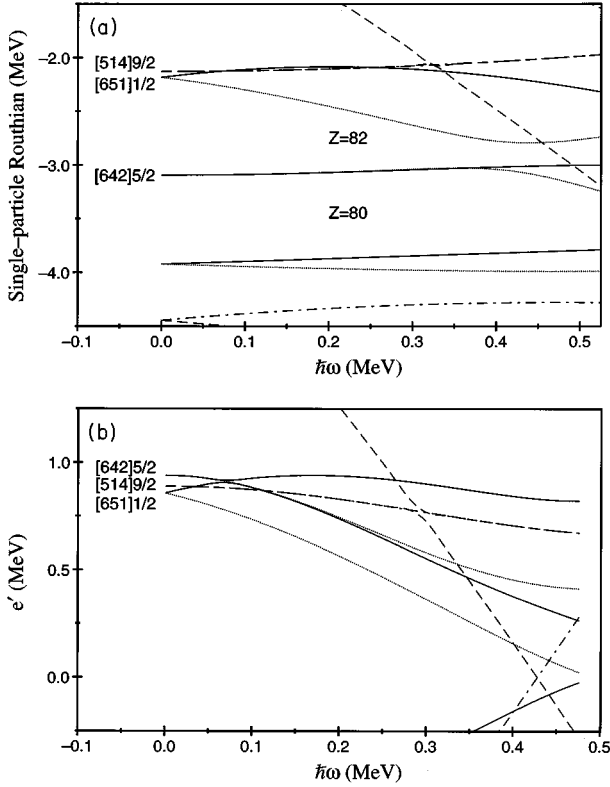


FIG. 6. (a) Cranked Woods-Saxon single-particle diagram for protons. The deformation parameters used were $\beta_2=0.48$, $\beta_4=0.07$, and $\gamma=0.0^\circ$. (b) Cranked Woods-Saxon quasiparticle diagram for protons. The deformation parameters used were the same as those above, while the pairing parameter was taken as $\Delta_p=\Delta_{\text{BCS}}(\omega=0)$. Parity and signature (π, α) of the levels are indicated in the following way: solid line= $(+, +1/2)$, dotted line= $(+, -1/2)$, dot-dashed line= $(-, +1/2)$, and dashed line= $(-, -1/2)$.

find evidence for a strongly coupled signature-partner sequence of similar intensity. Therefore, the lack of observation of signature-partner sequences for the bands in $^{195,197}\text{Bi}$ (bands 1 and 3, respectively) implies that the configurations of these bands probably do not involve the [642]5/2 orbital.

A similar argument applies for the [514]9/2 state which should give rise to a strongly coupled structure with $K=9/2$ [two signature partners with very little signature splitting and populated with similar intensities; note also that the strong coupling model predicts a large $B(M1)$ strength ($\sim 1.9\mu_N^2$) [30] which should lead to strong dipole “cross-talk” transitions between the two signature partner bands]. Furthermore, the two signature partners should have $\mathcal{J}^{(2)}$ moments of inertia similar to those of the yrast SD bands in the neighboring even-Pb core (^{194}Pb and ^{196}Pb for ^{195}Bi and ^{197}Bi , respectively) [31,32,23,33,34] since the intruder occupation is the same. None of these features are displayed by the bands we observe.

The [651]1/2 ($i_{11/2}$) level is the most plausible one-quasiproton excitation. This strongly aligned orbital is expected to exhibit immediate signature splitting with the $\alpha = -1/2$ partner being favored. As the rotational frequency increases the splitting is expected to increase [see Fig. 6(b)].

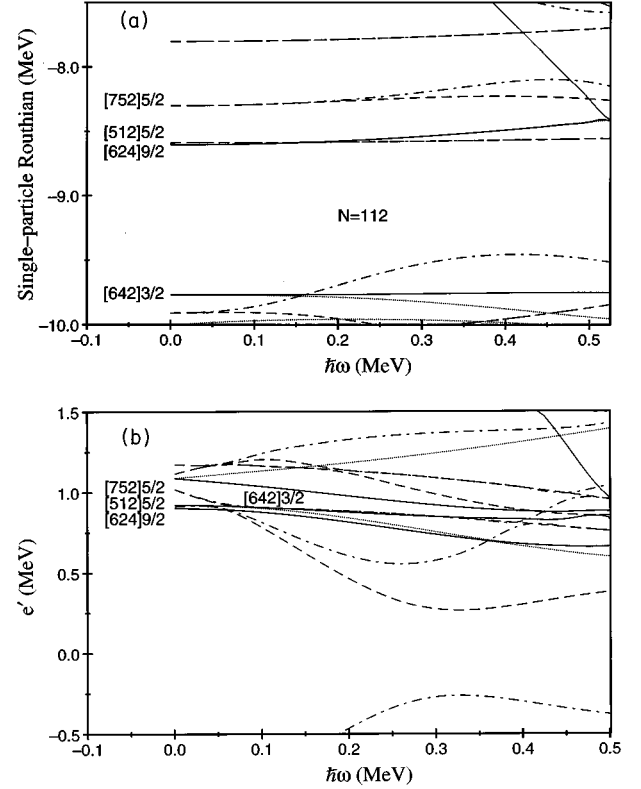


FIG. 7. (a) Cranked Woods-Saxon single-particle diagram for neutrons. (b) Cranked Woods-Saxon quasiparticle diagram for neutrons. The deformation parameters used were the same as those for Fig. 6. The pairing parameter for the quasiparticle diagram was taken as $\Delta_n=\Delta_{\text{BCS}}(\omega=0)$. Parity and signature are indicated in the same way as Fig. 6.

The SD band based on the favored signature of this orbital should be more intensely populated than the unfavored band. This provides an explanation for our observation of only one SD band in ^{195}Bi and ^{197}Bi . In addition, the alignment of this orbital is similar to that of the [642]5/2 levels. This provides a qualitative explanation for the observed similarity in the magnitude and slopes of the $\mathcal{J}^{(2)}$'s for the bands in the odd-Bi and odd-Tl isotopes (see Fig. 4). Therefore, from the above considerations, we propose that the bands observed in $^{195,197}\text{Bi}$ are based on this configuration.

For ^{196}Bi an odd proton and an odd neutron must be coupled to the even- ^{194}Pb core. Presumably the odd proton occupies the same [651]1/2 orbital as in the neighboring odd-Bi isotopes. As described in Sec. III, the band in ^{196}Bi (band 2) is the strongest SD band seen in the data and no unsplit signature partner band could be found, suggesting that this band can be associated with a strongly rotation-aligned neutron orbital. A single-particle Woods-Saxon calculation for neutrons, with the same deformation parameters as for the proton calculation [see Fig. 6(a)], is presented in Fig. 7(a). A quasineutron Routhian plot is shown in Fig. 7(b). Feasible one-quasineutron excitations involve the [512]5/2, [624]9/2, and [752]5/2 orbitals.

Bands based on the [512]5/2 and [624]9/2 levels have been observed in the isotones ^{193}Hg [35–37], ^{194}Tl [6], and ^{195}Pb [10]. They have been found to form, as expected from the calculation [see Fig. 7(b)], strongly coupled signature-

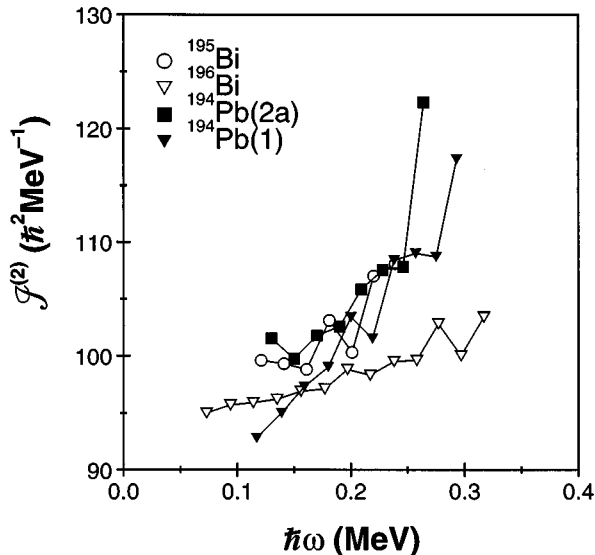


FIG. 8. Plot of the $\mathcal{J}^{(2)}$ moments of inertia as a function of rotational frequency for the SD bands in ^{194}Pb (bands 1 and 2a), ^{195}Bi , and ^{196}Bi .

partner pairs of bands with little signature splitting. (Dipole cross talk has also been observed between several pairs of these bands.) Clearly, this observation implies that the configuration of the band we see cannot involve either of these orbitals.

The $[752]5/2$ ($j_{15/2}$) orbital is predicted to be the most favored quasineutron excitation. Pronounced splitting between the two signatures of this $N=7$ level is predicted to occur with $\alpha = -1/2$ being favored. This is consistent with our observation of only one band. Note that in ^{195}Pb [10] ($Z=82$, $N=113$) it is the favored $N=7$ signature-partner band that is most intensely populated. The unfavored signature partner has only ≈ 0.5 the intensity of the favored band. Furthermore, the SD bands in ^{195}Pb which are based on the $N=7$ levels have very flat moments of inertia (a Pauli-blocking effect; see below). This is shown in Fig. 4 which plots the $\mathcal{J}^{(2)}$ of the ^{196}Bi band with that of the favored $N=7$ band of ^{195}Pb . This feature ties in with our observation of a much reduced slope of the $\mathcal{J}^{(2)}$ for the band assigned to ^{196}Bi . From these considerations we suggest that the band in ^{196}Bi is based on a configuration which may be represented as $^{194}\text{Pb}(\text{SD core}) \otimes \pi[651]1/2 \otimes \nu[752]5/2$.

Several important points can be made concerning the relative behavior of the $\mathcal{J}^{(2)}$'s of these bands. Figure 8 shows plots of the $\mathcal{J}^{(2)}$ moments of inertia for SD bands in ^{194}Pb , ^{195}Bi , and ^{196}Bi . We start by considering the steady rise in the $\mathcal{J}^{(2)}$ of the ^{194}Pb band 1 which is understood in terms of a smooth quasiparticle alignment due to $\nu j_{15/2}$ and $\pi i_{13/2}$ orbitals [3]. It is apparent from Fig. 8 that the $\mathcal{J}^{(2)}$ of the ^{195}Bi band is larger than that of $^{194}\text{Pb}(1)$ at lower frequencies and increases less rapidly with ω . This indicates that the presence of an unpaired proton close to the Fermi surface has blocked some of the proton pairing strength. The contribution to the rise in $\mathcal{J}^{(2)}$ from the alignment of the $i_{11/2}$ quasiprotons will be blocked, resulting in a small reduction in the slope with respect to $^{194}\text{Pb}(1)$. It is worth pointing out that the $\mathcal{J}^{(2)}$ of the excited bands in ^{194}Pb [23] [referred to as

$^{194}\text{Pb}(2a,2b)$ since they are thought to be a strongly coupled signature partner pair] have similar magnitudes and slopes to that of the band in ^{195}Bi . Indeed, as has already been pointed out, the band in ^{195}Bi has nearly identical transition energies to $^{194}\text{Pb}(2b)$. In [23] it was not possible to determine if the excited bands were based on a proton or neutron excitation; however, the similarity of the bands to that in ^{195}Bi is noteworthy, although the relationship of these bands is not clear. For ^{196}Bi both the $[651]1/2$ $i_{11/2}$ proton orbital and the $[752]5/2$ $j_{15/2}$ neutron orbital are occupied with an odd nucleon. At low rotational frequency this tends to raise the magnitude of $\mathcal{J}^{(2)}$ and the additional Pauli blocking of the $j_{15/2}$ quasineutron alignment results in a reduced slope. However, as can be seen in Fig. 4, the magnitude of the $\mathcal{J}^{(2)}$ for the ^{196}Bi band is smaller than that for the favored $N=7$ band of ^{195}Pb . The addition of a proton to the favored signature of the $[651]1/2$ orbital should not produce such a relative effect unless other factors such as differences in the pairing strengths and deformations for the two structures are also important.

V. SUMMARY AND FUTURE WORK

Two experiments have been performed using the ^{183}W ($^{19}\text{F},xn$) and $^{181}\text{Ta}(^{20}\text{Ne},xn)$ reactions at 108 and 123 MeV, respectively. The Gammasphere array was used to detect the emitted γ rays. Three SD bands are seen in the data, and one has been assigned to each of ^{195}Bi , ^{196}Bi , and ^{197}Bi , although the band assignments remain tentative. The properties of the bands in the odd-Bi nuclei are best reproduced if the odd proton occupies the $[651]1/2$ ($\alpha = -1/2$) orbital. The band in ^{196}Bi probably has this same proton configuration coupled to an additional $j_{15/2}$ neutron. The relative behavior of the $\mathcal{J}^{(2)}$'s of these bands can be understood in terms of Pauli-blocking effects. Our results represent important information on the nature of the proton orbitals above $Z=82$ at extreme deformation.

Important questions remain to be addressed. It is an experimental imperative to confirm the superdeformed nature of the bands through lifetime measurements. Additional experiments are required to search for excited SD bands in these Bi nuclei. In particular, the signature partners to the bands already observed need to be found. This will give more information on the nature and the strength of pairing correlations and on Pauli-blocking effects. In addition, strongly coupled signature-partner pairs of bands based on the $[514]9/2$ and $[642]5/2$ proton orbitals should exist. These bands should exhibit strong dipole cross talk and allow us to deduce g factors for these levels. These measurements, combined with what is already known for the SD bands in the Tl isotopes, should give us a complete picture of the nature of the proton orbitals close to the $Z=82$ SD subshell closure.

ACKNOWLEDGMENTS

The crew and staff of the 88-Inch Cyclotron are thanked. This work has been supported in part by the U.S. Department of Energy under Contract Nos. DE-AC03-76SF00098 (LBL) and W-7405-ENG-48 (LLNL), and by Research Corporation Grant No. R-152 (ISU).

- [1] E.F. Moore *et al.*, Phys. Rev. Lett. **63**, 360 (1989).
- [2] R.B. Firestone and B. Singh (unpublished).
- [3] M.A. Riley *et al.*, Nucl. Phys. **A512**, 178 (1990).
- [4] M.W. Drigert *et al.*, Nucl. Phys. **A530**, 452 (1991).
- [5] Y. Liang *et al.*, Phys. Rev. C **46**, R2136 (1992).
- [6] F. Azaiez *et al.*, Phys. Rev. Lett. **66**, 1030 (1991).
- [7] M.P. Carpenter *et al.* (unpublished).
- [8] M.J. Joyce *et al.*, Phys. Lett. B **340**, 150 (1994).
- [9] J.R. Hughes *et al.*, Phys. Rev. C **51**, R447 (1995).
- [10] L.P. Farris *et al.*, Phys. Rev. C (to be published).
- [11] R.R. Chasman, Phys. Lett. B **219**, 227 (1989).
- [12] W. Satula, S. Cwiok, W. Nazarewicz, R. Wyss, and A. Johnson, Nucl. Phys. **A529**, 289 (1991).
- [13] S.J. Krieger, P. Bonche, M.S. Weiss, J. Meyer, H. Flocard, and P.H. Heenen, Nucl. Phys. **A542**, 43 (1992).
- [14] R.M. Clark *et al.*, Phys. Rev. C **51**, R1052 (1995).
- [15] D. McNabb *et al.*, contribution to DNP meeting, Williamsburg, VA, 1994 (unpublished).
- [16] "GAMMASPHERE, A National Gamma-ray Facility," edited by M.A. Deleplanque and R.M. Diamond, Lawrence Berkeley Laboratory Report No. PUB-5202, 1988.
- [17] T. Lönnroth, C.W. Beausang, D.B. Fossan, L. Hildingsson, W.F. Piel, Jr., M.A. Quader, S. Vajda, T. Chapurán, and E.K. Warburton, Phys. Rev. C **33**, 1641 (1986).
- [18] A.H. Wapstra and K. Bos, At. Data Nucl. Data Tables **20**, 1 (1977).
- [19] T. Chapurán, K. Dybdal, D.B. Fossan, T. Lönnroth, W.F. Piel, Jr., D. Horn, and E.K. Warburton, Phys. Rev. C **33**, 130 (1986).
- [20] J.O. Newton, F.S. Stephens, and R.M. Diamond, Nucl. Phys. **A236**, 225 (1974).
- [21] P.B. Fernandez *et al.*, Nucl. Phys. **A517**, 386 (1990).
- [22] F. Azaiez *et al.*, Z. Phys. A **338**, 471 (1991).
- [23] J.R. Hughes *et al.*, Phys. Rev. C **50**, R1265 (1994).
- [24] F.S. Stephens *et al.*, Phys. Rev. Lett. **64**, 2623 (1990).
- [25] F.S. Stephens *et al.*, Phys. Rev. Lett. **65**, 301 (1990).
- [26] P. Fallon, contribution to the Conference on Physics from Large γ -ray Detector Arrays, Berkeley, 1994 (unpublished).
- [27] W. Nazarewicz, R. Wyss, and A. Johnson, Nucl. Phys. **A503**, 285 (1989).
- [28] J. Duprat *et al.*, Phys. Lett. B **341**, 6 (1994).
- [29] S. Bouneau *et al.* (unpublished).
- [30] P.B. Semmes, I. Ragnarsson, and S. Aberg, Phys. Rev. Lett. **68**, 460 (1992).
- [31] K. Theine *et al.*, Z. Phys. A **336**, 113 (1990).
- [32] M.J. Brinkman *et al.*, Z. Phys. A **336**, 115 (1990).
- [33] E.F. Moore *et al.*, Phys. Rev. C **48**, 2261 (1993).
- [34] T.F. Wang *et al.*, Phys. Rev. C **43**, R2465 (1991).
- [35] D.M. Cullen *et al.*, Phys. Rev. Lett. **65**, 1547 (1990).
- [36] P. Fallon *et al.*, Phys. Rev. Lett. **70**, 2690 (1993).
- [37] M.J. Joyce *et al.*, Phys. Rev. Lett. **71**, 2176 (1993).